Effects of energetic disorder and diffusion on the hole transport in the TQ1:$PC_{71}BM$ photovoltaic blends

L. H. LUO, L. G. WANG*, Y. L. LIANG, L. ZHANG, Y. J. WANG
School of Electrical Engineering and Automation, Henan Key Laboratory of Intelligent Detection and Control of Coal Mine Equipment, Henan Polytechnic University, Jiaozuo, 454000, People's Republic of China

In this paper, the hole transport and spatial correlations between the transport site energies in the TQ1:$PC_{71}BM$ (poly[[2,3-bis(3-octyloxyphenyl)-5,8-quinoxalinediyl]-2,5-thiophenediyl]:[6,6]-phenyl C71 butyric acid methyl ester) blends as used in organic photovoltaics are investigated. From an analysis of the temperature-dependent current density-voltage ($J-V$) characteristics of the TQ1:$PC_{71}BM$ hole-only device, it is found that consistent descriptions with equal quality can be obtained using both the improved extended Gaussian disorder model (IEGDM) and the extended correlated disorder model (ECDM). However, the intersite distance obtained using IEGDM is more realistic than the value obtained using ECDM, which indicates that in the TQ1:$PC_{71}BM$ blends, the correlations between the transport site energies are absent. Based on a comparison between analyses of the $J-V$ characteristics of the TQ1:$PC_{71}BM$ hole-only device using IEGDM and the drift-diffusion simulations incorporating the extended correlated disorder model (DD+EGDM), it is demonstrated that the diffusion has little effect on the charge transport in the TQ1:$PC_{71}BM$ blends. In addition, it is shown that the effective mobility in the TQ1:$PC_{71}BM$ blends gradually increases with increasing temperature, and the maximum value of the carrier concentration and the minimum value of the field strength appear at the interface of the TQ1:$PC_{71}BM$ hole-only device.

(Received March 31, 2022; accepted August 10, 2022)

Keywords: Organic photovoltaics, Hole transport, Correlated disorder, Drift-diffusion

1. Introduction

In recent years, the entire field of organic solar cells has developed by leaps and bounds, and a series of important progress has been made in material design and synthesis, device preparation optimization, device physical mechanism and lifetime. Organic photovoltaics (OPVs) have the advantages of low production cost, high flexibility, light weight and easy processing. It has great development potential and is expected to provide the next generation of energy [1-3]. Many research groups and laboratories in the field have achieved photoelectric power conversion efficiency (PCE) of more than 15% [4-7]. The most advanced device structure is based on a bulk heterojunction (BHJ) formed by a mixture of electron donors and electron acceptors. The interface characteristics of the BHJs play a vital role in exciton dissociation and charge transfer, which control the performance of the organic devices [8-12]. Polymer:fullerene TQ1:$PC_{71}BM$ (poly[[2,3-bis(3-octyloxyphenyl)-5,8-quinoxalinediyl]-2,5-thiophenediyl]:[6,6]-phenyl C71 butyric acid methyl ester) yields a PCE of 7% and displays a high internal-quantum efficiency of ≈90% [13, 14], which represents a useful model system for BHJ organic photovoltaics featuring effective charge generation and transport. The positive integer charge state of TQ1 is equal in energy to the negative integer charge state of $PC_{71}BM$, leading to a negligible potential step at TQ1:$PC_{71}BM$ interface and thus the vacuum level alignment [15]. As a result, TQ1:$PC_{71}BM$ is an ideal system for a detailed investigation of the charge transport in the organic photovoltaic blends.

Charge carrier transport in disordered organic semiconductors is commonly understood to occur by incoherent hopping of charge carriers between molecular sites with random energies. The most important parameter characterizing the transport is the charge carrier mobility. Due to the typically Gaussian distribution of site energies, the mobility becomes strongly dependent on temperature T, charge carrier density p, and electrostatic field E. In the past two decades, various methods have been proposed to calculate the mobility function [16-23]. The pioneering work of Bässler et al. used kinetic Monte Carlo (kMC) simulation, and the random energy is described by Gaussian Density of States (DOS), leading to the Gaussian disorder model (GDM) [16], which only considers the low-density Boltzmann limit and shows discrepancies in the field dependence that are attributed to spatial correlations of the site energies [17, 18]. In addition, some people think that the spatial correlation of site energy is caused by the interaction of charge and dipole [19], leading to the correlated disorder model (CDM). Later, it

was realized that, apart from the dependence of the mobility on the electric field and temperature, there is also a strong dependence on the carrier density p [20-23], leading to the extended Gaussian disorder model (EGDM) and extended correlated disorder model (ECDM) [20, 21], within which spatial correlations between the transport site energies are absent and are included, respectively. Recently, it has been suggested that a more physical approach as drift-diffusion (DD) modeling can be used to simulate the whole OPV device including contacts and active layer, and can reproduce steady-state experimental data by incorporating the EGDM [24]. However, the EGDM, only having a non-Arrhenius temperature dependence $\ln(\mu) \propto 1/T^2$, cannot well describe the charge transport at high carrier densities [25]. To date, it is still unclear which models can provide the better descriptions for the charge transport in disordered organic semiconductors.

In this paper, the hole transport and possible presence of spatially correlated disorder in the TQ1:$PC_{71}BM$ blends are investigated. Firstly, we perform a detailed analysis of the temperature dependence of the current density-voltage ($J-V$) characteristics of hole-only device based on the TQ1:$PC_{71}BM$ blends by using the IEGDM and ECDM. Subsequently, we re-analyse the temperature dependent $J-V$ characteristics using the drift-diffusion simulations incorporating the EGDM (DD+EGDM), and investigate the effect of diffusion on the charge transport in the TQ1:$PC_{71}BM$ blends. Finally, the variation of $J-V$ characteristics with the boundary carrier density, and the distribution of carrier density and electric field with the distance from the interface of the TQ1:$PC_{71}BM$ hole-only device are given.

2. Models and methods

The simple analytical GDM model does not account for the dependence of the mobility on charge carrier concentration and applied field. In order to characterize charge transport more accurately in disordered organic semiconductors, the use of numerical simulations is required. A well-established mobility model that includes the effects of temperature, charge concentration, and electric field on the mobility is the extended Gaussian disorder model (EGDM) [20]. This model describes the mobility in the situation of hopping transport in a system with a Gaussian density of states distribution, given by

$$\mu(T,p,E) \approx \mu_0(T)\, f(T,E) \exp\left[\frac{1}{2}\left(\hat{\sigma}^2-\hat{\sigma}\right)\left(2pa^3\right)^{\delta}\right], \quad (1)$$

$$\mu_0(T) = \mu_0 b_1 \exp(-b_2\hat{\sigma}^2), \quad (2a)$$

$$f(T,E) = \exp\left\{0.44\left(\hat{\sigma}^{3/2}-2.2\right)\left[\sqrt{1+0.8\left(\frac{eaE}{\sigma}\right)^2}-1\right]\right\}. \quad (2b)$$

Where $\mu_0(T)$ is the mobility in the limit of zero carrier density and electric field, $b_1 = 1.8\times10^{-9}$, $b_2 = 0.42$, $\hat{\sigma} \equiv \sigma / k_B T$ is the reduced disorder, σ is the width of Gaussian density of states (DOS), e is the charge of the carriers, a is the lattice constant and ν_0 is the attempt-to-hop frequency.

It should be noted that the EGDM, only having a non-Arrhenius temperature dependence $\ln(\mu) \propto 1/T^2$, cannot well describe the charge transport at high carrier densities. In order to better describe the charge transport, we proposed an improved model within which the temperature dependence of the mobility based on both the non-Arrhenius temperature dependence and Arrhenius temperature dependence $\ln(\mu) \propto 1/T$, leading to the improved extended Gaussian disorder model (IEGDM) [26]. The dependence of the zero-field mobility on the carrier density p and temperature T is given by

$$\mu(T,p) = \mu_0(T)\exp\left[\frac{1}{2}\left(\hat{\sigma}^2-\hat{\sigma}\right)\left(2pa^3\right)^{\delta}\right], \quad (3a)$$

$$\mu_0(T) = \mu_0 c_1 \exp(c_2\hat{\sigma} - c_3\hat{\sigma}^2), \quad (3b)$$

$$\delta \equiv 2\frac{\ln(\hat{\sigma}^2-\hat{\sigma}) - \ln(\ln 4)}{\hat{\sigma}^2}, \quad \mu_0 \equiv \frac{a^2\nu_0 e}{\sigma}, \quad (3c)$$

where $c_1 = 0.48\times10^{-9}$, $c_2 = 0.80$, and $c_3 = 0.52$. The field dependence of the mobility is included via

$$\mu(T,p,E) = \mu(T,p)^{g(T,E)} \exp\left[c_4\left(g(T,E)-1\right)\right], \quad (4)$$

$$g(T,E) = \left[1 + c_5 (Eea/\sigma)^2\right]^{-1/2}, \quad (5)$$

where $g(T,E)$ is a weak density dependent function, c_4 and c_5 are weak density dependent parameters, given by

$$c_4 = d_1 + d_2 \ln(pa^3) \quad (6a)$$

$$c_5 = 1.16 + 0.09\ln(pa^3) \quad (6b)$$

$$d_1 = 28.7 - 36.3\hat{\sigma}^{-1} + 42.5\hat{\sigma}^{-2} \quad (7a)$$

$$d_2 = -0.38 + 0.19\hat{\sigma} + 0.03\hat{\sigma}^2 \quad (7b)$$

In addition to uncorrelated energetic disorder, the presence of molecular dipoles may give rise to spatial correlations in the energy distribution of the sites. Bouhassoune et al. employed the same methodology as in the EGDM, but for an energy landscape with Gaussian disorder that result from randomly oriented dipole moments of equal magnitude on all lattice sites, leading to the extended correlated disorder model (ECDM) [21]. The mobility can be described as follows:

$$\mu(T,p,E)=[(\mu_{low}(T,p,E))^{q(\hat{\sigma})}+(\mu_{high}(p,E))^{q(\hat{\sigma})}]^{1/q(\hat{\sigma})}, \tag{8}$$

$$q(\hat{\sigma})=2.4/(1-\hat{\sigma}), \tag{9}$$

with $\mu_{low}(T,p,E)$ the mobility in the low-field limit, and with $\mu_{high}(p,E)$ the mobility in the high-field limit.

$$\mu_{low}(T,p,E)=\mu_0(T)g(T,p)f(T,E,p) \tag{10}$$

where $g(T,p)$ and $f(T,E,p)$ are the dimensionless mobility enhancement functions. These functions can be written as follows:

$$\mu_0(T)=1.0\times10^{-9}\mu_0\exp(-0.29\hat{\sigma}^2), \tag{11}$$

$$g(T,p)=\begin{cases}\exp[(0.25\hat{\sigma}^2+0.7\hat{\sigma})(2pa^3)^{\delta}], pa^3<0.025\\ g(T,0.025a^{-3}), pa^3\geq0.025\end{cases}, \tag{12}$$

$$\delta\equiv2.3\frac{\ln(0.5\hat{\sigma}^2+1.4\hat{\sigma})-0.327}{\hat{\sigma}^2}, \tag{13}$$

$$f(T,E_{red},p)=\exp[h(E_{red})(1.05-1.2(pa^3)^{r(\hat{\sigma})})(\hat{\sigma}^{3/2}-2)(\sqrt{1+2E_{red}}-1)] \tag{14}$$

$$h(E_{red})=1,\ \ r(\hat{\sigma})=0.7\hat{\sigma}^{-0.7}, \tag{15}$$

within the very low-field, $0\leq E_{red}<0.16\equiv E^*_{red}$, $h(E_{red})$ can be written as

$$h(E_{red})=\begin{cases}\frac{4}{3}\frac{E_{red}}{E^*_{red}}, (E_{red}\leq E^*_{red}/2)\\ \left[1-\frac{4}{3}\left(\frac{E_{red}}{E^*_{red}}-1\right)^2\right], (E^*_{red}/2\leq E_{red}\leq E^*_{red})\end{cases} \tag{16}$$

$$\mu_{high}(p,E)=\frac{2.06\times10^{-9}}{E_{red}}\mu_0(1-pa^3)\cdot \tag{17}$$

Using the above model and the following coupled equations, the $J-V$ characteristics of organic electron devices can be exactly calculated by employing a particular uneven discretization method introduced in our previous papers [27, 28].

$$J=p(x)e\mu(T,p(x),E(x))E(x), \tag{18a}$$

$$\frac{dE}{dx}=\frac{e}{\varepsilon_0\varepsilon_r}p(x), \tag{18b}$$

$$V=\int_0^L E(x)dx, \tag{18c}$$

where x is the distance from the injecting electrode, ε_0 is the vacuum permeability, ε_r is the relative dielectric constant of the organic semiconductors, and L is the organic semiconductor layer thickness sandwiched between two electrodes.

3. Results and discussion

To explore the charge transport in more detail and evaluate the energetic disorder, we investigate the temperature dependence of the hole current in the TQ1:$PC_{71}BM$ blends. Figs. 1 and Fig. 2 show the $J-V$ characteristics of a hole-only organic electronic device with a thickness of 110 nm based on the TQ1:$PC_{71}BM$ at different temperatures. The solid lines in Fig.1 and Fig.2 represent the numerical calculation results of IEGDM and ECDM combined with the coupled equations (Eqs.(18)), and the symbol is the experimental data of the $J-V$ characteristics [23]. It can be seen from the figures that the numerical calculation results of the organic electronic device based on the IEGDM and ECDM models are quite consistent with the experimental data. In the IEGDM and ECDM models, the charge transport is described by the three input parameters: the width of Gaussian density of state distribution σ, the intersite distance a, and a mobility prefactor μ_0. The mobility prefactor μ_0 is a temperature-independent parameter that only influences the magnitude of the mobility, σ mainly controls the temperature and charge concentration dependence of the mobility, and a predominantly affects the field dependence of the mobility. The three parameters in IEGDM and ECDM are $a=1.7$ nm, $\sigma=0.099$ eV, $\mu_0=20$ m^2/Vs, and $a=0.32$ nm, $\sigma=0.126$ eV, $\mu_0=50$ m^2/Vs, respectively. It is found that the best-fit values of the intersite distance a as obtained from the

IEGDM and ECDM are quite different. The value of a found for the ECDM may be considered as unrealistically small (significantly lower than the typical value of organic semiconductors), in view of the fact that in copolymer TQ1 the use of side-chain architecture is expected to give rise to a larger typical distance between neighboring polymer chains in the TQ1:PC_{71}BM blends [29]. Furthermore, intra-chain hopping between the rather long segments is also expected to be associated with larger a. However, the value of a obtained from the IEGDM is very close to the typical value of organic semiconductors, and slightly smaller than the value obtained by Melianas et al. for the TQ1:PC_{71}BM blends (1.8 nm) [30]. These results indicate that there is no correlation between transport site energy in the TQ1:PC_{71}BM blends. The comparison between the values obtained for σ and μ_0 does not change this point of view. For disordered organic semiconductors, the width of the DOS is typically observed to fall in the range 0.06-0.15 eV. It is thus clear that the optimal values of σ obtained from the IEGDM and ECDM in the present study (0.099 ev for the IEGDM and 0.126 ev for the ECDM) are physically realistic.

To compare the applicability of the IEGDM with EGDM and investigate the effect of diffusion on the charge transport in the TQ1:PC_{71}BM blends, we re-analyse the above temperature dependent $J-V$ characteristics using the EGDM by also taking the diffusion contribution to the current density into account. The experimental data is fitted with drift-diffusion simulations incorporating the EGDM (DD+EGDM), using an energetic disorder σ of 0.0922 eV and a lattice constant a of 1.75 nm, as displayed in Fig. 3. As can be observed in this figure, the experimental $J-V$ curves cannot be well described by using drift-diffusion simulations incorporating the EGDM (especially in low voltage range), even though taking both the drift and diffusion contribution to the current into account. However, it can be seen from Fig. 1 that the experimental data can be well fitted over the full voltage range by the IEGDM in the case of only taking the effect drift on the current density into account. Therefore, it is concluded that the diffusion has little effect on the charge transport in the TQ1:PC_{71}BM blends. The above results show that, compared with the EGDM and ECDM, the IEGDM can better describe the charge transport in the TQ1:PC_{71}BM blends.

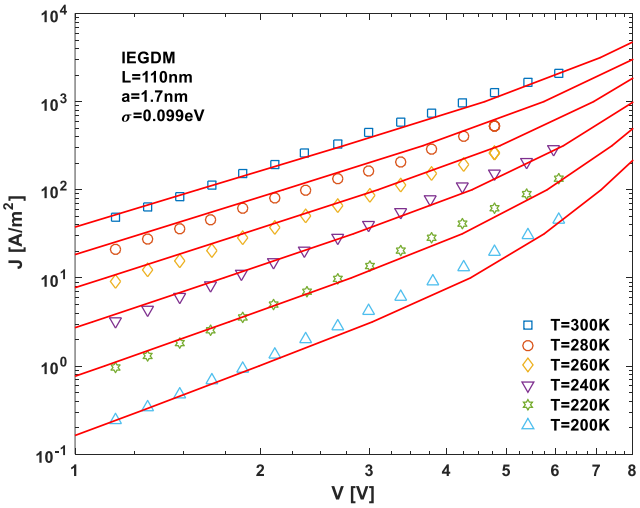

Fig. 1. Temperature dependent $J-V$ characteristics of a hole-only device based on TQ1:PC_{71}BM 1:1 with a layer thickness of 110 nm. Symbols are experimental data from Ref. [23]. Lines are the numerically calculated results based on the IEGDM (color online)

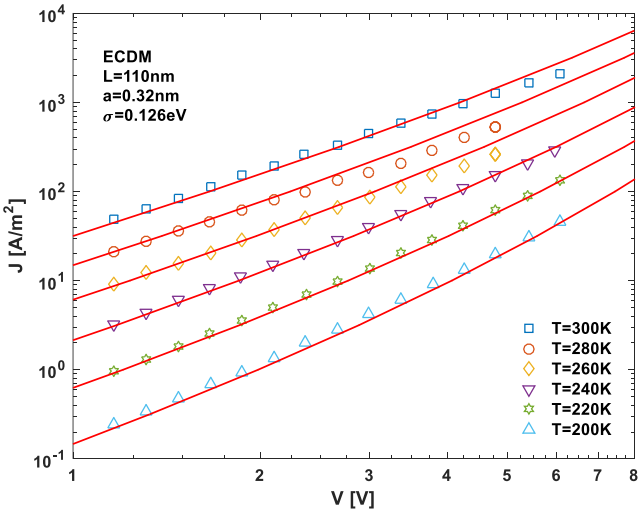

Fig. 2. Temperature dependent $J-V$ characteristics of a hole-only device based on TQ1:PC_{71}BM 1:1 with a layer thickness of 110 nm. Symbols are experimental data from Ref. [23]. Lines are the numerically calculated results based on the ECDM (color online)

Finally, we will use IEGDM and the numerical methods described in Sec.2 to systematically study the electrical properties of the TQ1:PC_{71}BM blends. Fig.4 shows the variations of $J-V$ characteristic with the boundary carrier concentration *p(0)* for TQ1:PC_{71}BM hole-only device at low temperature and at room temperature. The figure shows that the voltage increases with increasing the current density, and the variation of voltage with *p(0)* is dependent on the current density. In

the density range of 10^{23}–10^{25} m^{-3}, the *V - p(0)* curves are fairly flat, indicating that the voltage is independent of *p(0)* and the *J - V* characteristics are physically realistic in this region. On the other hand, the voltage decreases with increasing *p(0)* for *p(0)* less than 10^{23} m^{-3}, and also increases with increasing *p(0)* for *p(0)* more than 10^{25} m^{-3}. Furthermore, it can be seen from the figure that in order to reach the same current density J at the same *p(0)*, the stronger electric field and the corresponding larger voltage are needed at low temperature than those at room temperature. This can be explained by the fact that the effective mobility as determined at room temperature is higher than that at low temperature.

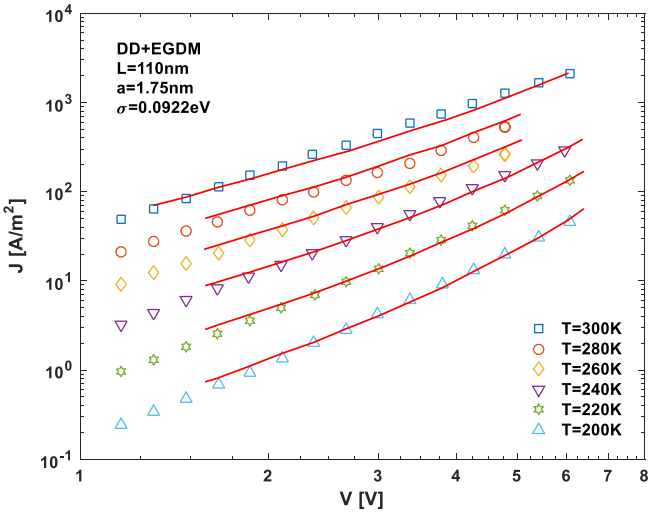

Fig. 3. Temperature dependent $J-V$ characteristics of a hole-only device based on TQ1:$PC_{71}BM$ 1:1 with a layer thickness of 110 nm. Symbols are experimental data from Ref. [23]. Lines are the numerically calculated results based on the DD+EGDM (color online)

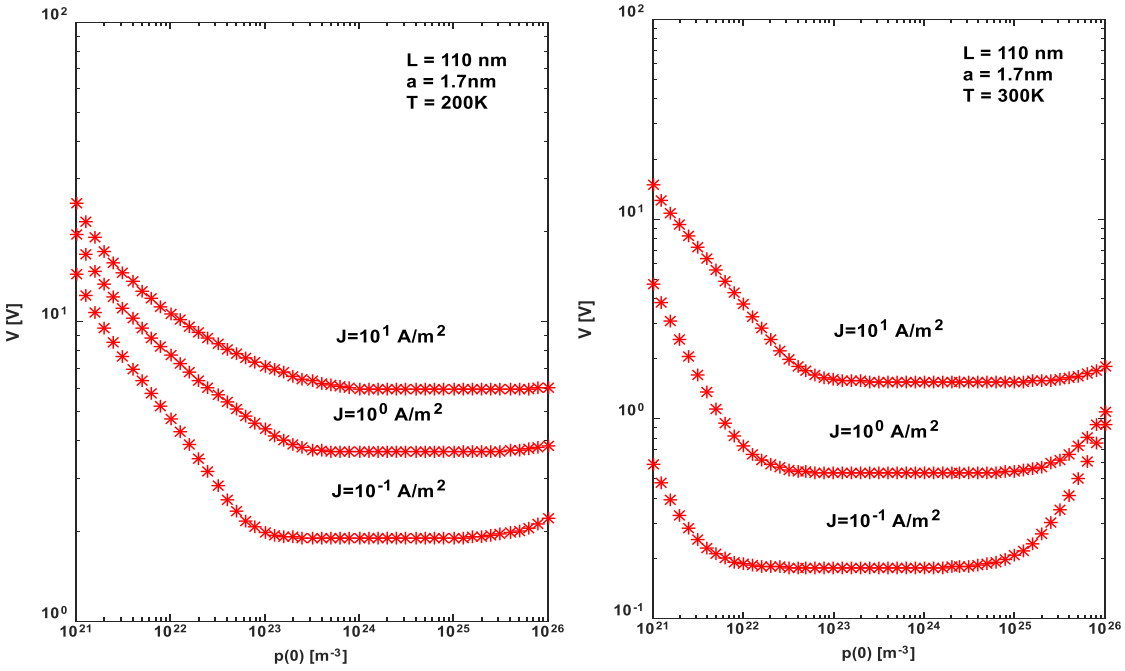

Fig. 4. Theoretical results of voltage versus the boundary carrier density of a hole-only device based on TQ1:$PC_{71}BM$ blends at 200 K and 300 K (color online)

The numerically calculated distribution of the carrier density and electric field as a function of the distance from the interface of TQ1:$PC_{71}BM$ hole-only device at low temperature and at room temperature are plotted in Fig. 5. It can be seen from the figure that the carrier density *p(x)* is a decreasing function of the distance, and the electric

field *E(x)* is an increasing function of the distance X. The function of *p(x)* with a relatively large *p(0)* decreases faster than that with a relatively small *p(0)*. On the other hand, the function of *E(x)* with a relatively small *p(0)* increases faster than that with a relatively large *p(0)*. As the distance X increases, *p(x)* in the organic semiconductor film rapidly reaches saturation. The thickness of accumulation layer decreases with increasing *p(0)*. The variation of carrier density *p(x)* and electric field *E(x)* with the distance X at low temperature (200 K) is greater than that at room temperature (300 K), which further indicates that the effective mobility at room temperature is higher than that at low temperature. Both the maximum of carrier concentration and the minimum of electric field appear near the interface of TQ1:PC_{71}BM hole-only device. As a result, the injection of carriers from the electrode into the TQ1:PC_{71}BM organic layer leads to carriers accumulation near the interface and a decreasing function *p(x)*. The distribution of *p(x)* leads to the variation of *E(x)*, and the carriers accumulation near the interface results in increasing function *E(x)*.

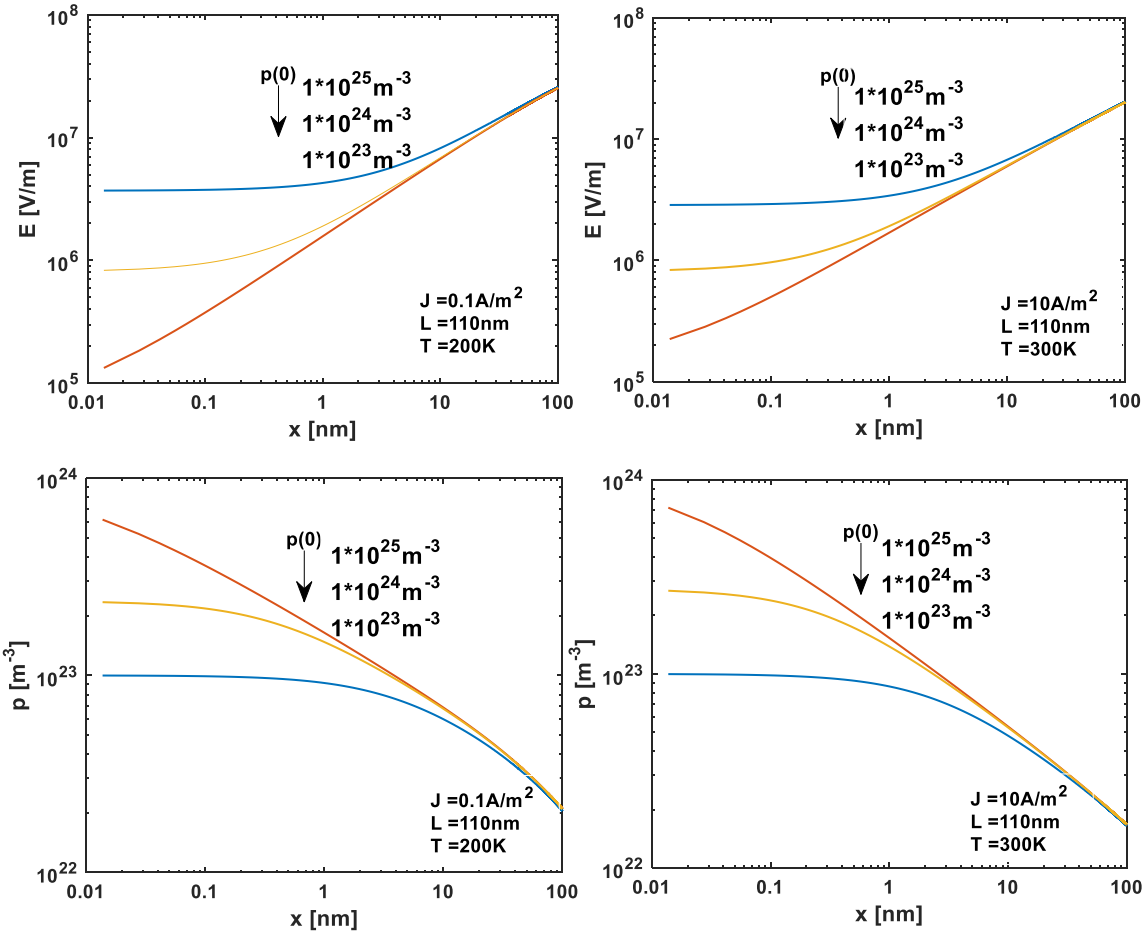

Fig. 5. Numerically calculated distribution of the charge carrier density p and electric field E as a function of the distance X in a hole-only device based on TQ1:PC_{71}BM blends at 200 K and 300 K (color online)

4. Summary and conclusions

In summary, the effects of energetic disorder and diffusion on the hole transport in the TQ1:PC_{71}BM photovoltaic blends are studied. It is found that consistent descriptions with equal quality for the temperature dependent $J-V$ characteristics of the TQ1:PC_{71}BM hole-only device can be obtained using both the IEGDM and ECDM. However, the intersite distance obtained using IEGDM is more realistic than the value obtained using ECDM, which indicates that the correlations between the transport site energies in the TQ1:PC_{71}BM blends are absent. The comparison between DD+EGDM and IEGDM proves that the diffusion has little effect on the charge transport in the TQ1:PC_{71}BM blends. In addition, it is shown that the effective mobility in the TQ1:PC_{71}BM blends gradually increases with increasing temperature. These numerical results show that, compared with the EGDM and ECDM, the IEGDM can better describe the charge transport in disordered organic semiconductors.

Acknowledgements

This work is supported by the Fundamental Research Funds for the Universities of Henan Province Grant No. NSFRF200304 and No. NSFRF210424, the Science and Technology Project of Henan Province No. 202102210295, the Young Key Teacher Program of Henan Polytechnic University Grant No. 2019XQG-17, and the Doctoral Scientific Research Foundation of Henan Polytechnic University Grant No. B2014-022 and No. B2017-20.

References

[1] Y. Ie, K. Morikawa, W. Zajaczkowski, W. Pisula, N. B. Kotadiya, G. A. H. Wetzelaer, P. W. M. Blom, Y. Aso, Adv. Energy Mater. **8**, 1702506 (2018).
[2] N. B. Kotadiya, P. W. M. Blom, G. A. H. Wetzelaer, Phys. Rev. Applied **11**, 024069 (2019).
[3] T. Upreti, Y. Wang, H. Zhang, D. Scheunemann, F. Gao, M. Kemerink, Phys. Rev. Applied **12**, 064039 (2019).
[4] B. Fan, D. Zhang, M. Li, W. Zhong, Z. Zeng, L. Ying, F. Huang, Y. Cao, Sci. China Chem. **62**, 746 (2019).
[5] Y. Cui, H. Yao, L. Hong, Adv. Mater. **31**, 1808356 (2019).
[6] X. Xu, K. Feng, Z. Bi, Adv. Mater. **31**, 1901872 (2019).
[7] J. Yuan, L. Zhang, Joule **3**, 1141 (2019).
[8] H. Zhang, R. C. Shallcross, N. Li, T. Stubhan, Y. Hou, W. Chen, T. Ameri, M. Turbiez, N. R. Armstrong, C. J. Brabec, Adv. Energy Mater. **6**, 1502195 (2016).
[9] R. A. Street, Adv. Mater. **28**, 3814 (2016).
[10] H. Ishii, K. Sugiyama, E. Ito, K. Seki, Adv. Mater. **11**, 605 (1999).
[11] K. Vandewal, S. Albrecht, E. T. Hoke, K. R. Graham, J. Widmer, J. D. Douglas, Nat. Mater. **13**, 63 (2014).
[12] Q. Y. Bao, X. J. Liu, E. G. Wang, J. F. Fang, F. Gao, S. Braun, M. Fahlman, Adv. Mater. Interfaces. **2**, 1500204 (2015).
[13] Z. Tang, Z. George, Z. Ma, J. Bergqvist, K. Tvingstedt, K. Vandewal, E. Wang, L. M. Andersson, M. R. Andersson, F. Zhang, O. Inganas, Adv. Energy Mater. **2**, 1467 (2012).
[14] Y. Kim, H. R. Yeom, J. Y. Kim, C. Yang, Energy Environ. Sci. **6**, 1909 (2013).
[15] Q. Bao, X. Liu, S. Braun, Solar RRL **1**, 1700142 (2017).
[16] H. Bässler, Phys. Status Solidi B **175**, 15 (1993).
[17] S. V. Novikov, D. H. Dunlap, V. M. Kenkre, P. E. Parris, A. V. Vannikov, Phys. Rev. Lett. **81**, 4472 (1998).
[18] M. Bouhassoune, S. L. M. van Mensfoort, P. A. Bobbert, R. Coehoorn, Org. Electron. **10**, 437 (2009).
[19] Y. N. Gartstein, E. M. Conwell, Chem. Phys. Lett. **245**, 351 (1995).
[20] W. F. Pasveer, J. Cottaar, C. Tanase, R. Coehoorn, P. A. Bobbert, P. W. M. Blom, D. M. de Leeuw, M. A. J. Michels, Phys. Rev. Lett. **94**, 206601 (2005).
[21] M. Bouhassoune, S. L. M. van Mensfoort, P. A. Bobbert, R. Coehoorn, Org. Electron. **10**, 437 (2009).
[22] S. D. Baranovskii, Phys. Status Solidi A **215**, 1700676 (2018).
[23] N. Felekidis, A. Melianas, M. Kemerink, Org. Electron. **61**, 318 (2018).
[24] N. Felekidis, A. Melianas, M. Kemerink, Phys. Rev. B **94**, 035205 (2016)
[25] N. I. Craciun, J. Wildeman, P. W. M. Blom, Phys. Rev. Lett. **100**, 056601 (2008).
[26] L. G. Wang, H. W. Zhang, X. L. Tang, C. H. Mu, Eur. Phys. J. B **74**, 1 (2010).
[27] L. G. Wang, H. W. Zhang, X. L. Tang, Y. Q. Song, Optoelectron. Adv. Mat. **5**, 263 (2011).
[28] M. L. Liu, L. G. Wang, J. Optoelectron. Adv. M. **19**, 406 (2017).
[29] E. Wang, J. Bergqvist, K. Vandewal, Z. Ma, L. Hou, A. Lundin, S. Himmelberger, A. Salleo, C. Müller, O. Inganas, F. Zhang, M. R. Andersson, Adv. Energy Mater. **3**, 806 (2013).
[30] A. Melianas, V. Pranculis, Y. Xia, N. Felekidis, O. Inganas, V. Gulbinas, M. Kemerink, Adv. Energy Mater. **7**, 1602143 (2017).

*Corresponding author: wangliguo@hpu.edu.cn